

X-810-72-227

PREPRINT

NASA TMX-65948

SIMULTANEOUS L-BAND AND VHF IONOSPHERIC FADING EFFECTS AT THE GEOMAGNETIC EQUATOR

(NASA-TM-X-65948) SIMULTANEOUS L-BAND AND
VHF IONOSPHERIC FADING EFFECTS AT THE
GEOMAGNETIC EQUATOR (NASA) 20 P HC

\$3.00

CSCL 20N

N73-21173

G3/07

Unclas
68263

APRIL 1972



GODDARD SPACE FLIGHT CENTER
GREENBELT, MARYLAND

SIMULTANEOUS L-BAND AND VHF IONOSPHERIC
FADING EFFECTS AT THE
GEOMAGNETIC EQUATOR

W. B. Sessions*
and T. S. Golden
Network Engineering Division

April 1972

*Westinghouse Electric Corporation, P.O. Box 1693, Baltimore, Maryland 21203

GODDARD SPACE FLIGHT CENTER
Greenbelt, Maryland

SIMULTANEOUS L-BAND AND VHF IONOSPHERIC
FADING EFFECTS AT THE GEOMAGNETIC
EQUATOR*

T. S. Golden
Network Engineering Division
and
W. B. Sessions

ABSTRACT

Simultaneous observations of ionospheric fading of 1550-MHz and 136-MHz radio waves from the ATS-5 spacecraft were recorded on the geomagnetic equator at Ancon, Peru. The observations were made during a period around the 1971 spring equinox; they show fades as great as 27 dB at 136 MHz, and 6 dB at 1550 MHz.

The general characteristics of the scintillation signatures at the two frequencies are discussed with emphasis on comparison of the two frequencies with respect to rates and depths of fades. Typical statistical distributions of signal levels are also presented from which time availabilities of the signals relative to the median levels can be derived.

*Presented at the International Union of Radio Science (URSI) 1972 Spring Meeting, April 13-15, 1972

CONTENTS

	<u>Page</u>
INTRODUCTION	1
EXPERIMENT DESCRIPTION	2
EXPERIMENT RESULTS	2
CONCLUSIONS	3
REFERENCES	4

ILLUSTRATIONS

<u>Figure</u>		<u>Page</u>
1	Percent of VHF Minitrack Passes Subject to Ionospheric Scintillation Fading at Quito, Ecuador Averaged for Each Hour Time Block by Week	6
2	Percent of VHF Minitrack Passes Subject to Ionospheric Scintillation Averaged Over 12 Months at Fairbanks, Alaska; Quito, Ecuador; Lima, Peru; and Santiago, Chile	7
3	Basic Propagation Experiment and Data-Processing Flow . .	8
4	Ionospheric Disturbance of VHF and L-Band Signals	9
5	Hours and Peak-to-Peak Range of Ionospheric Scintillation Observed at Ancon, Peru During the 1971 Spring Equinox (sheet 1 of 2)	10
	Hours and Peak-to-Peak Range of Ionospheric Scintillation Observed at Ancon, Peru During the 1971 Spring Equinox (sheet 2 of 2)	11
6	L-Band and VHF Scintillation Records Received from ATS 5	12

Preceding page blank

ILLUSTRATIONS (Continued)

<u>Figure</u>		<u>Page</u>
7	Cumulative Amplitude Distribution of ATS-5 L-Band and VHF Signals	13
8	Cumulative Amplitude Distribution of ATS-5 and INTELSAT-1 Signals	14
9	L-Band and VHF Distributions	15

SIMULTANEOUS L-BAND AND VHF IONOSPHERIC FADING EFFECTS AT THE GEOMAGNETIC EQUATOR

INTRODUCTION

Since the advent of artificial earth satellites, a problem of concern to NASA has been the degradation of telemetry data quality due to effects of the equatorial ionosphere. The problem is thought to be a result of the inhomogeneous structure of the ionosphere giving rise to scintillation or fluctuation of electromagnetic waves propagating through the ionosphere. Scintillation effects have been observed across a broad range of frequencies, particularly at VHF (136 MHz), L-Band (1550 MHz), and S-Band (1700 and 2200 MHz) channels.

Several observers have established that VHF scintillation is notably more severe near the geomagnetic poles and the geomagnetic equator.^{1,2,3,4} Observations of VHF satellite records at Fairbanks, Alaska, from January 1965 to September 1967, showed occurrences of scintillation fading up to 30 dB.² In the equatorial region, VHF scintillation effects commonly exhibit fading occurrences of 25 dB. However, in the equatorial zone there is a seasonal and diurnal character to scintillation. The effects at the equator are more severe around the equinoxes and also occur predominantly during the evening hours. Figure 1⁵ shows plots of data for all Minitrack passes scheduled at Quito, Ecuador, from July 1966 through June 1967. The percent of passes for which scintillations occurred is plotted for 52 weeks as a function of time of day (GMT). At Quito, local midnight occurs at 0500 GMT. The seasonal and diurnal effect of scintillation is obvious. Figure 2⁵ shows the number of VHF scintillation events reported in all Minitrack passes for a 12-month period at four tracking stations at different latitudes. The equatorial zone shows strong diurnal trends with nighttime peaks, and the auroral zone has significant around-the-clock scintillation. The latitudinal behavior is also indicated.

Severe amplitude fluctuation at S-band (2200 MHz) has also been observed on signals received from the Apollo Lunar Surface Experiment Package (ALSEP). Analysis of data available for the period November 19, 1969 through June 30, 1970, shows signal fluctuations as large as 25 dB.⁶ The geographical, seasonal, and diurnal trends noted at VHF were also observed at S-band.

As a result of transionospheric propagation anomalies, Goddard Space Flight Center (GSFC) undertook studies to determine the impact of ionospheric irregularities on spacecraft communications. Through cooperation of the Applications Technology Satellite (ATS) Project Office, a propagation experiment using ATS 5

has been conducted with the specific intent of determining the severity of L-band scintillation in the equatorial regions and its relationship to VHF behavior.

EXPERIMENT DESCRIPTION

Figure 3 shows the basic propagation experiment. Simultaneous L-band (1550 MHz) and VHF (136 MHz) signals were received on the geomagnetic equator at Ancon, Peru (geographical coordinates $11^{\circ} 46' \text{ S}$, $76^{\circ} 52' \text{ W}$), from the ATS-5 spacecraft during March 11, 1971 through April 9, 1971. The time of day of the observations was restricted to evening and early morning hours. These observation times correspond to the expected times of VHF scintillation occurrence, and were specifically selected to maximize the probability of taking data when scintillation could be observed.

Figure 4 shows the two recorded signals. The VHF signal is a continuous carrier. However, difficulties encountered during insertion of the ATS-5 spacecraft into orbit resulted in ATS 5 spinning about an axis approximately parallel with the earth's axis and with a spin period of about 787 milliseconds. As a result, the L-band signal is received in energy pulsations for 52 milliseconds (3 dB points) as the spacecraft antenna pattern sweeps across the ground receiving system.

The data collected on magnetic tape were processed by automated techniques at GSFC using an IBM-360/91 computer. The amplitude calibrations in each data channel are automatically detected in the data processing and the information used to assign the proper magnitude to each data sample. The data is then processed to determine the frequency distribution and the cumulative distribution of the signal level for both the L-band and VHF signals.

The VHF data is sampled at a 5-millisecond rate; each data point is used to determine the VHF statistics. Due to the pulsating nature of the L-band signal (as seen in Figure 4), the amplitude of each L-band sample was determined and the peak values at the center of the beam were used in computing the L-band statistics.

EXPERIMENTAL RESULTS

Figure 5 (sheets 1 and 2) is a summary of all the observation times during the 1971 spring equinox. L-band scintillations with peak-to-peak magnitudes of greater than 3 dB occurred on 7 of the 24 days over which data was collected. Some L-band variations occurred with peak-to-peak amplitudes of 6 dB. These

scintillations generally occurred during periods of severe VHF scintillation. The noted maximum VHF scintillation exceeded the equipment dynamic range which implies values greater than 30 dB.

Figure 6 shows three records of simultaneous VHF and L-band scintillations. The top record shows that the onset of scintillation is generally abrupt, a fact noted by other observers.¹ Cessation also occurs in a sudden manner. Throughout the observations, it was noted that L-band scintillation is always accompanied by VHF scintillation. The top record (Figure 6) shows that the beginning and cessation of the L-band scintillation occurred simultaneously with the beginning and ending of VHF scintillation, indicating that the same physical mechanism may be responsible for scintillation at both frequencies. The center record (Figure 6) shows a change in state of the VHF scintillation at approximately 19:44 hours. The change is from large-amplitude slow-rate variations to somewhat smaller amplitude, faster rate variations. Note that, although the VHF amplitude variations decreased, the L-band scintillation activity increased. Throughout the observations, it was noted that during the most active L-band scintillation periods, the VHF rate was generally similar to that shown in the top and bottom records; and after 19:44 hours it was similar to that on the center record of Figure 6. Thus, the L-band activity appears to be associated with the rate of VHF scintillations.

Figure 7 shows a cumulative distribution of VHF and L-band signals during periods of scintillation. This distribution is typical of those observed during the 1971 spring equinox. Scintillation data was also collected on 24 days during the 1970 fall equinox. Figure 8 is a typical cumulative distribution of amplitude fading during this period. Distributions for the two time periods are very similar. Figure 9 shows a frequency distribution for both frequencies. These distributions are typical of those computed for all runs. The L-band distribution shows a small but measurable deviation. The VHF distribution is skewed toward the lower power levels.

CONCLUSIONS

Several observations and conclusions can be made regarding ionospheric scintillation in the equatorial regions. A summary of the findings follows:

- Microwave fading occurred to a measurable degree
- L-band fading statistics were generated for 26 1-hour samples during two equinox periods

- Peak-to-peak L-band signal fluctuations up to 6 dB were observed
- L-band fading was always accompanied by VHF fading
- L-band fading occurred 73 percent of the time that VHF fading was present
- Change of state (e. g., onset, etc.) of L-band fading was usually abrupt, similar to established VHF fading characteristics
- L-band fading amplitude was greater when VHF fading rate was high
- Over 1 hour, L-band signal levels fall, typically, 1.1 dB below the median for 1.0 percent of the time and 1.8 dB below the median for 0.1 percent of the time

The statistical behavior for L-band and VHF scintillation over the worst months of a year are described for the equatorial region. These statistics show that the amplitude of L-band scintillation is large enough to influence the design of highly reliable systems operating in the equatorial regions.

REFERENCES

1. J. Aarons, H. E. Whitney, and R. S. Allen. Global Morphology of Ionospheric Scintillations. Proc IEEE. Vol. 59, No. 2. Feb. 1971. p. 159-172
2. R. J. Coates and T. S. Golden. Ionospheric Effects of Telemetry and Tracking Signals from Orbiting Spacecraft. GSFC X-520-68-76. March 1968
3. E. J. Fremouw. Aberrations of VHF-UHF Signals Traversing the Auroral Ionosphere. Contract NAS 5-3940. Geophysical Institute. University of Alaska, College, Alaska. Final Report, August 1966
4. E. J. Fremouw and C. L. Rino. Development of a Worldwide Model for F-Layer-produced Scintillation. SRI Project 1079. Final Report. Nov. 1971

5. T. S. Golden. A Brief Review of Ionospheric Scintillation Fading Effects as Observed in NASA Satellite Tracking and Data Acquisition Networks. AIAA Paper No. 72-220. 10th Aerospace Sciences Meeting. San Diego, California. January 1972
6. R. M. Christiansen. Preliminary Report of S-Band Propagation Disturbance During ALSEP Mission Support (November 19, 1969 - June 30, 1970). GSFC X-861-71-239. June 1971

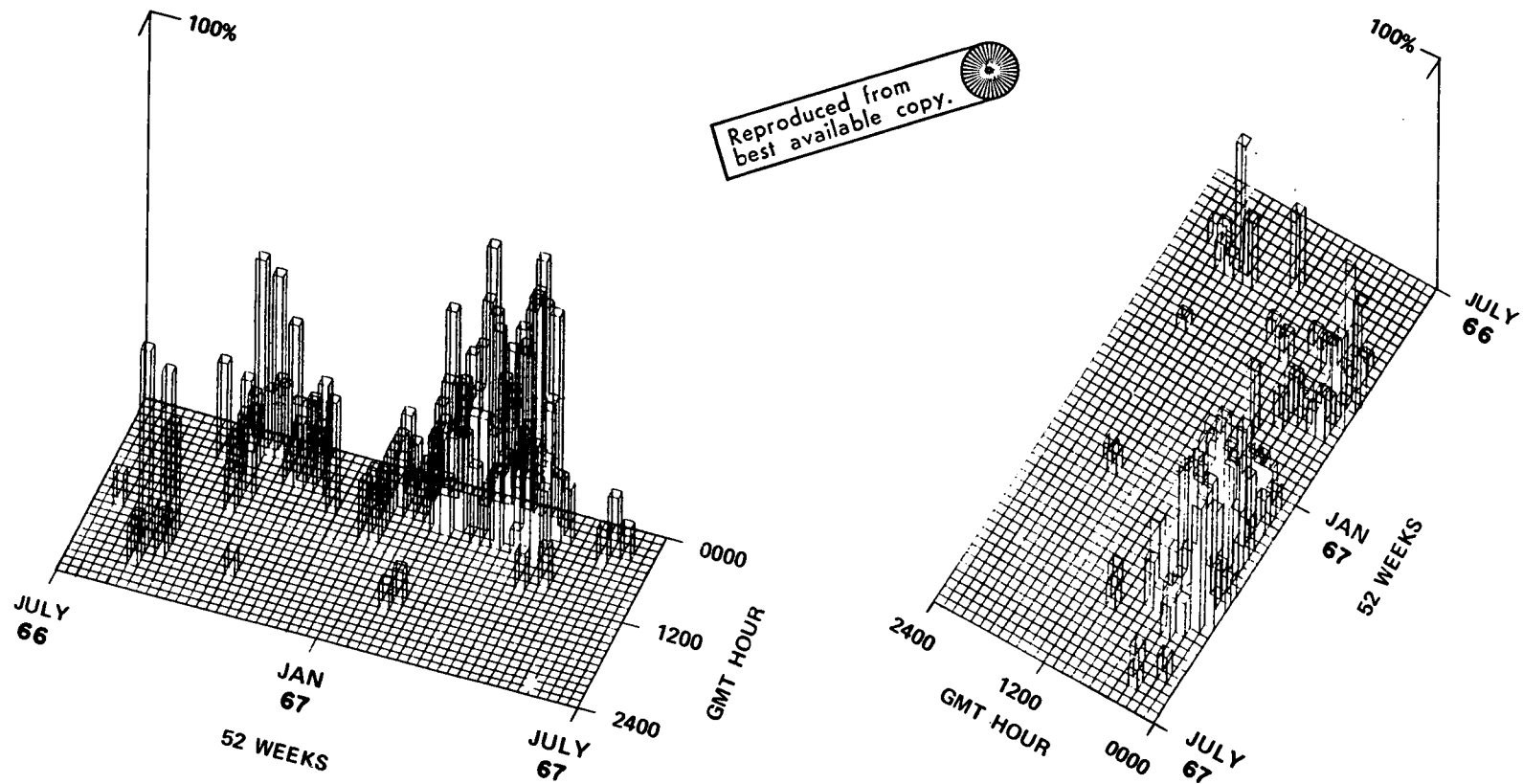


Figure 1. Percent of VHF Minitrack Passes Subject to Ionospheric Scintillation Fading at Quito, Ecuador Averaged for Each Hour Time Block by Week

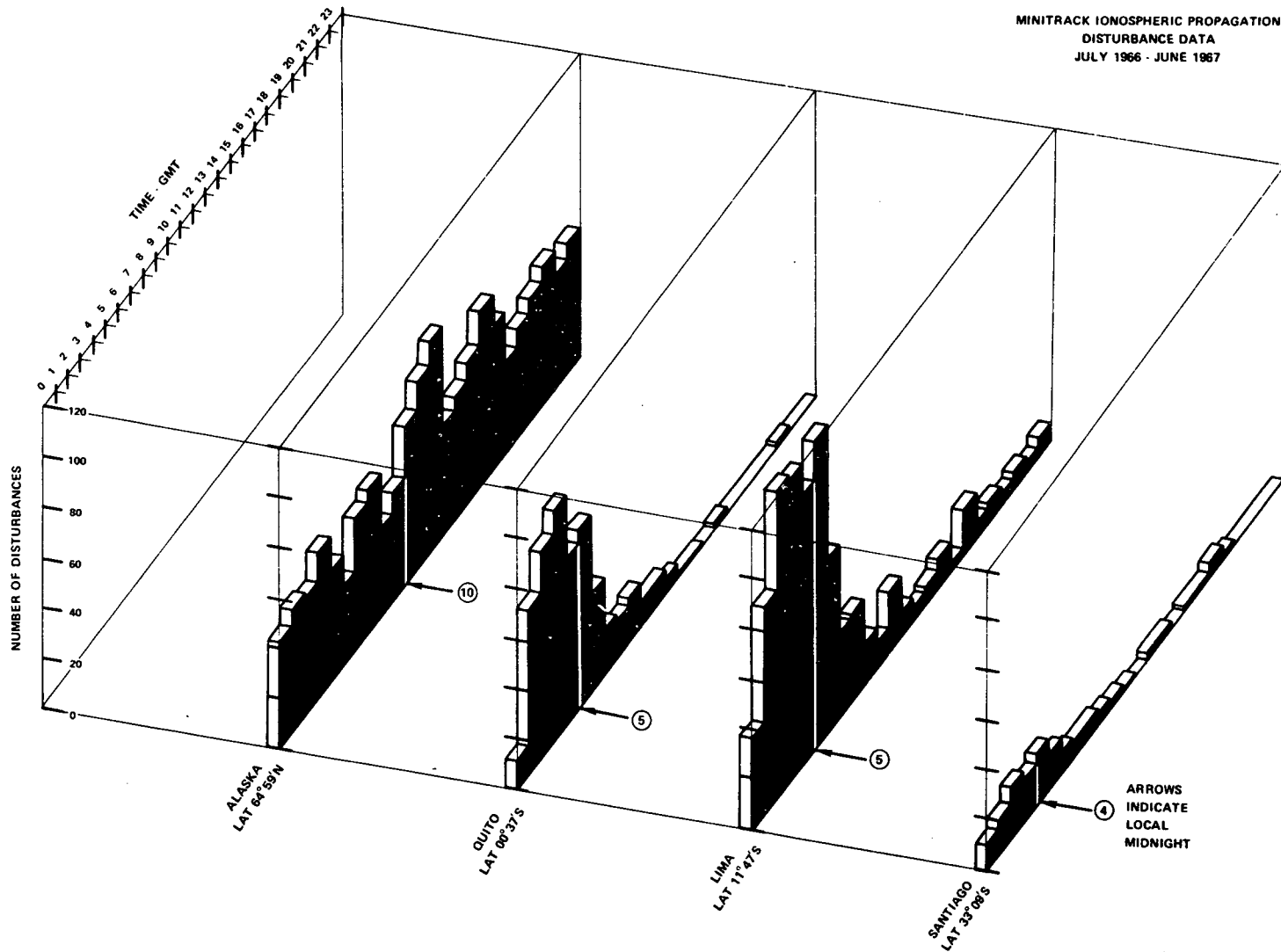


Figure 2. Percent of VHF Minitrack Passes Subject to Ionospheric Scintillation Averaged Over 12 Months at Fairbanks, Alaska; Quito, Ecuador; Lima, Peru; and Santiago, Chile

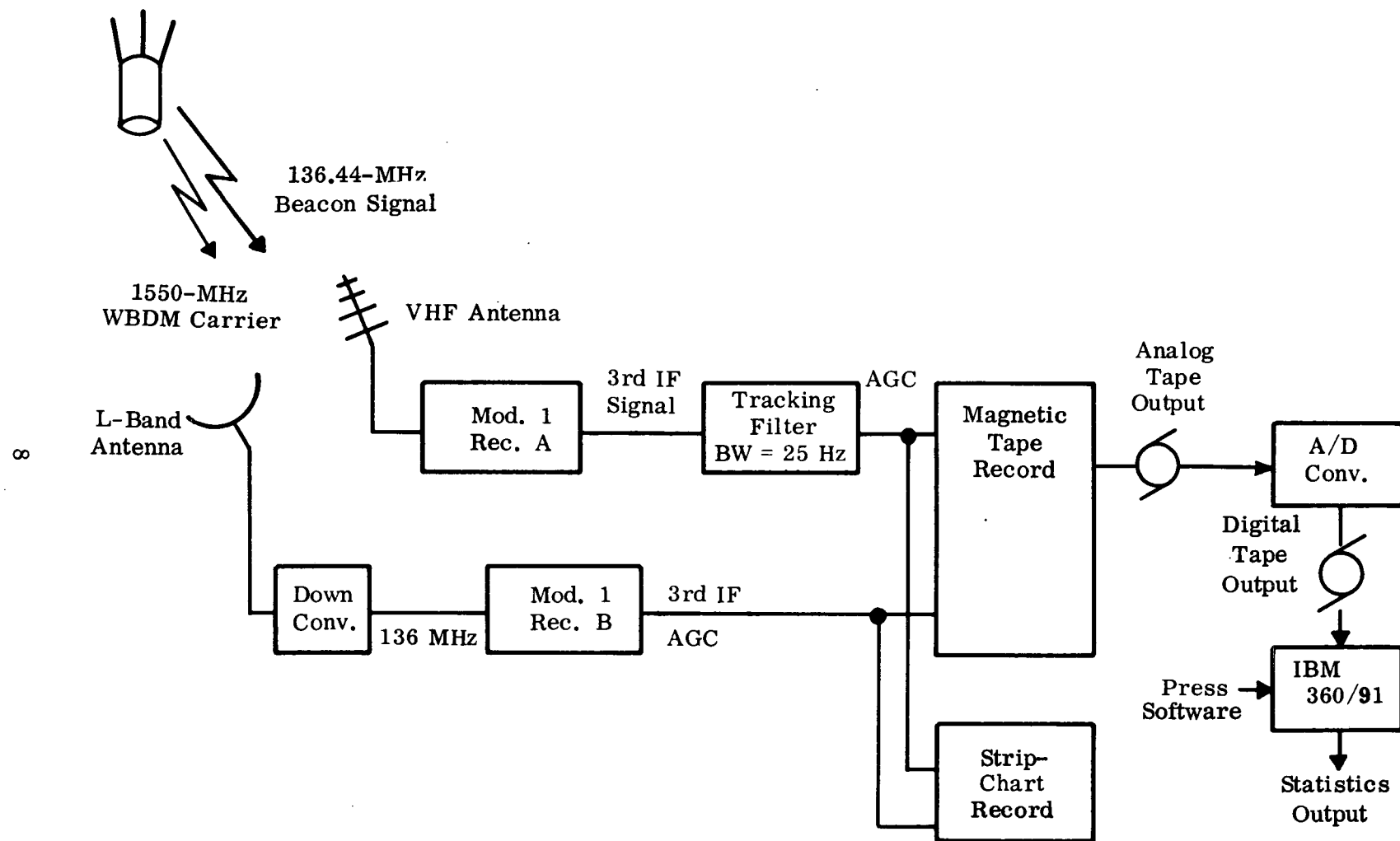


Figure 3. Basic Propagation Experiment and Data-Processing Flow

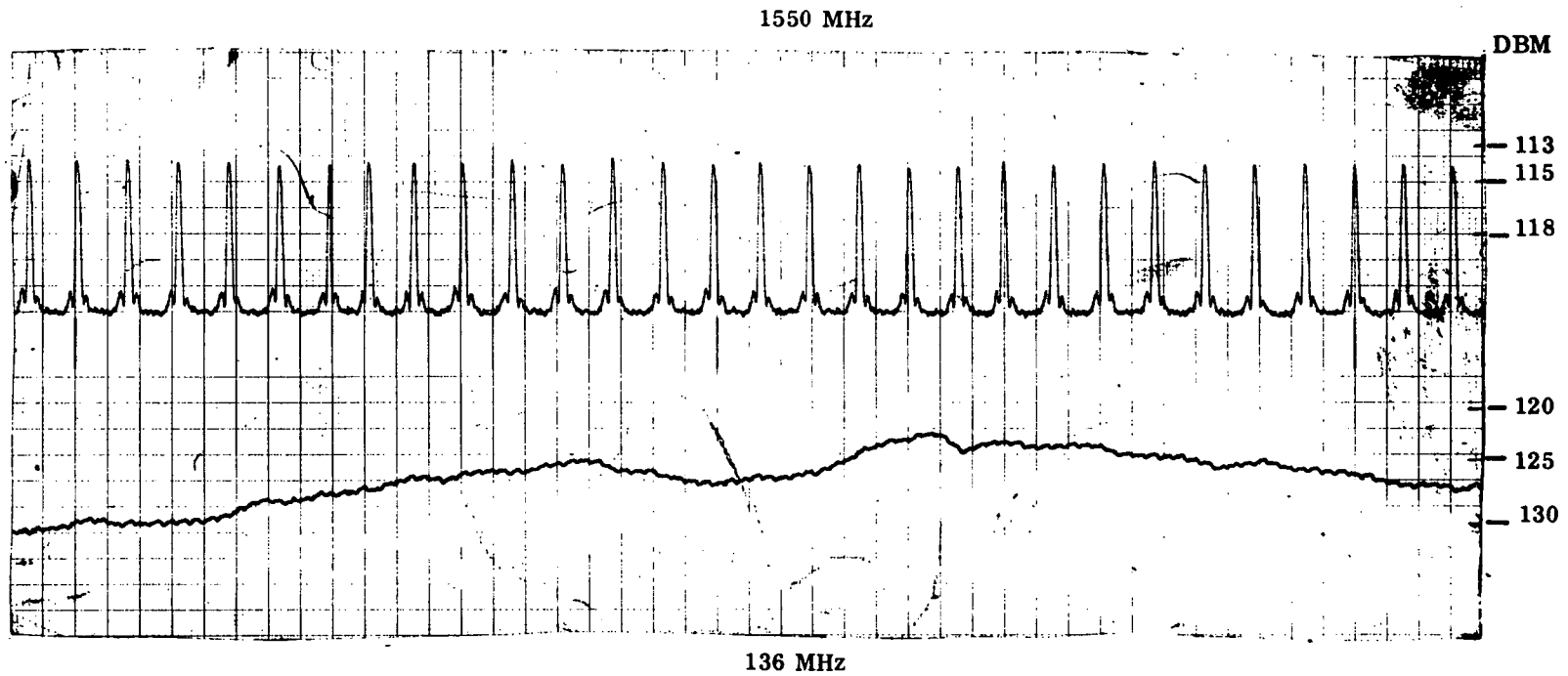


Figure 4. Ionospheric Disturbance of VHF and L-Band Signals

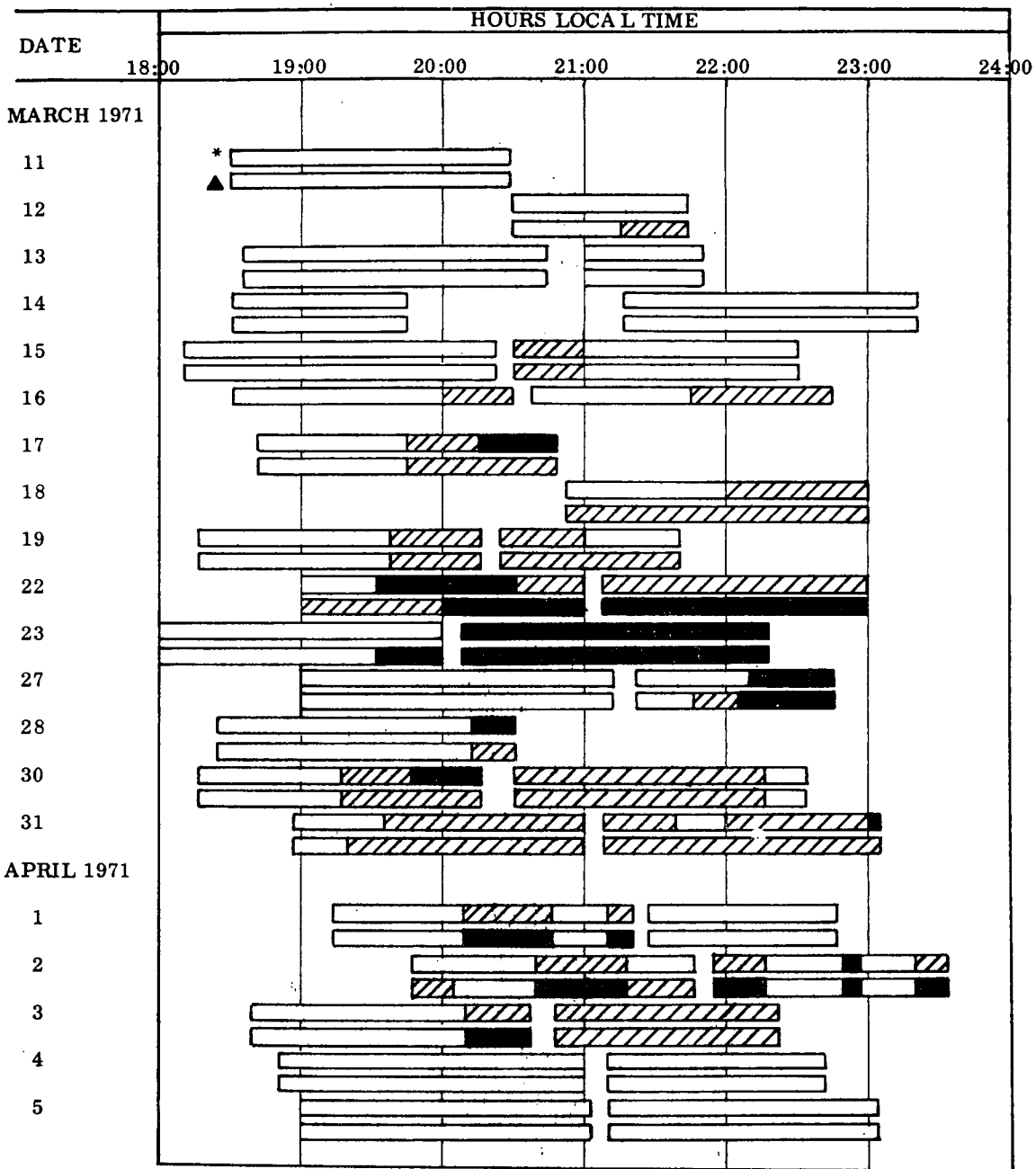
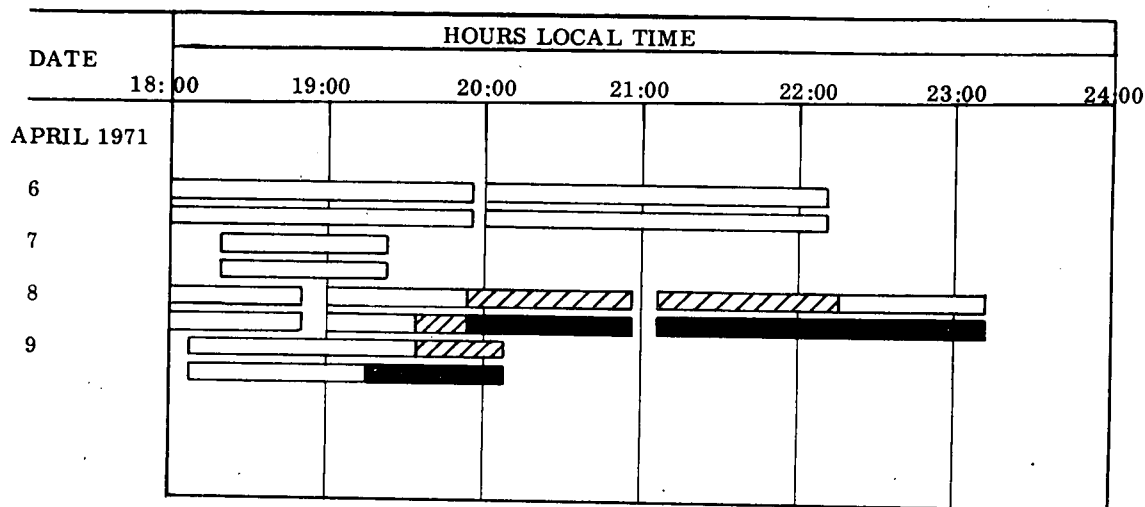


Figure 5. Hours and Peak-to-Peak Range of Ionospheric Scintillation Observed at Ancon, Peru During the 1971 Spring Equinox (sheet 1 of 2)



LEGEND




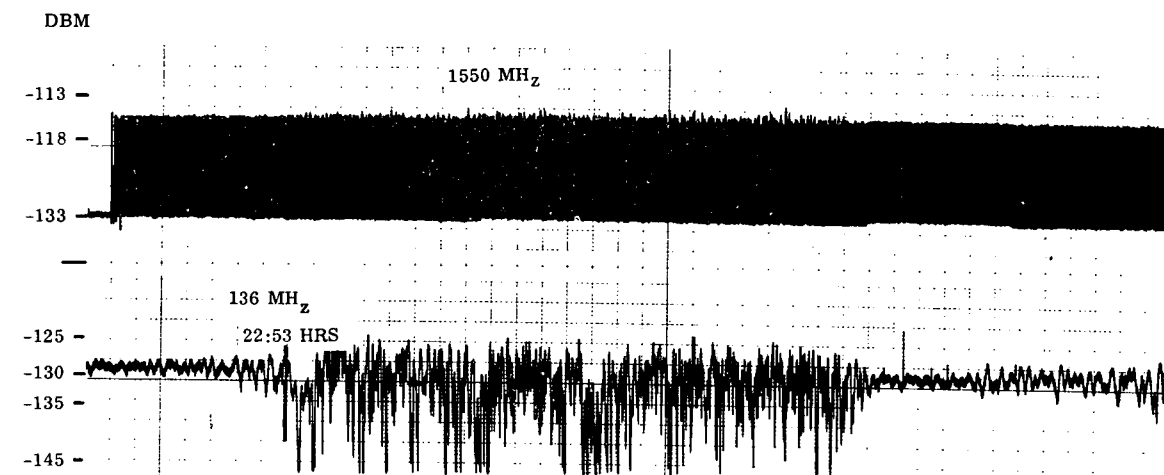
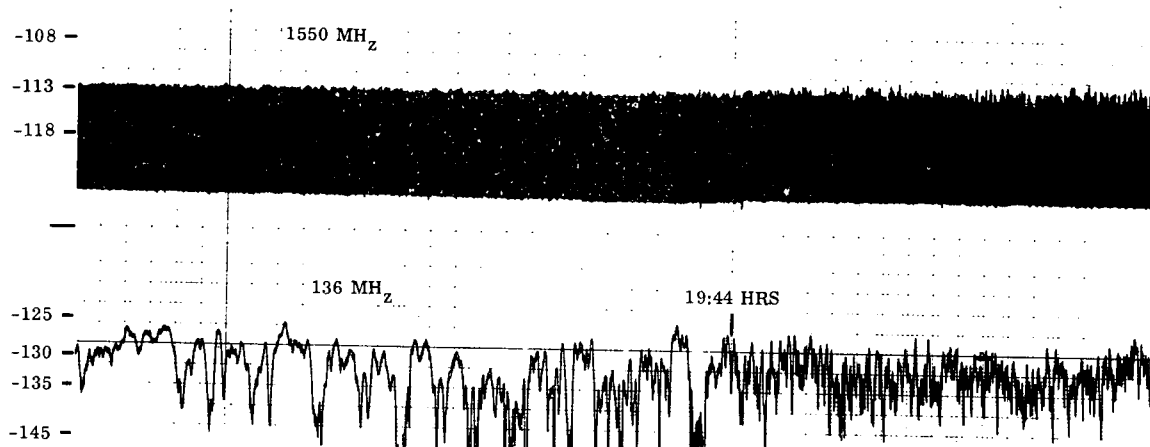
SYMBOL	L-BAND	VHF
	< 1	< 2
	1 - 3	2 - 10
	> 3	> 10
RANGE OF SCINTILLATION IN dB PEAK-TO-PEAK		
* L-BAND DATA		
▲ VHF DATA		

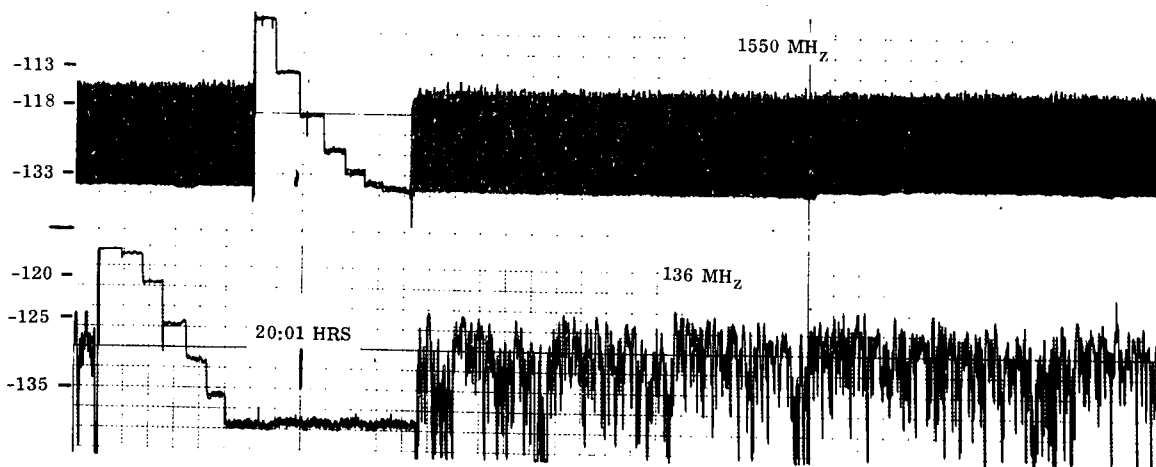
Figure 5. Hours and Peak-to-Peak Range of Ionospheric Scintillation Observed at Ancon, Peru During the 1971 Spring Equinox (sheet 2 of 2)



SCINTILLATION OCCURRENCE ON MARCH 22, 1971: TAPE SPEED = 80 sec/cm TIME →



SCINTILLATION OCCURRENCE ON APRIL 3, 1971: TAPE SPEED = 80 sec/cm TIME →



SCINTILLATION OCCURRENCE ON APRIL 2, 1971: TAPE SPEED = 80 sec/cm TIME →

Figure 6. L-Band and VHF Scintillation Records Received from ATS 5

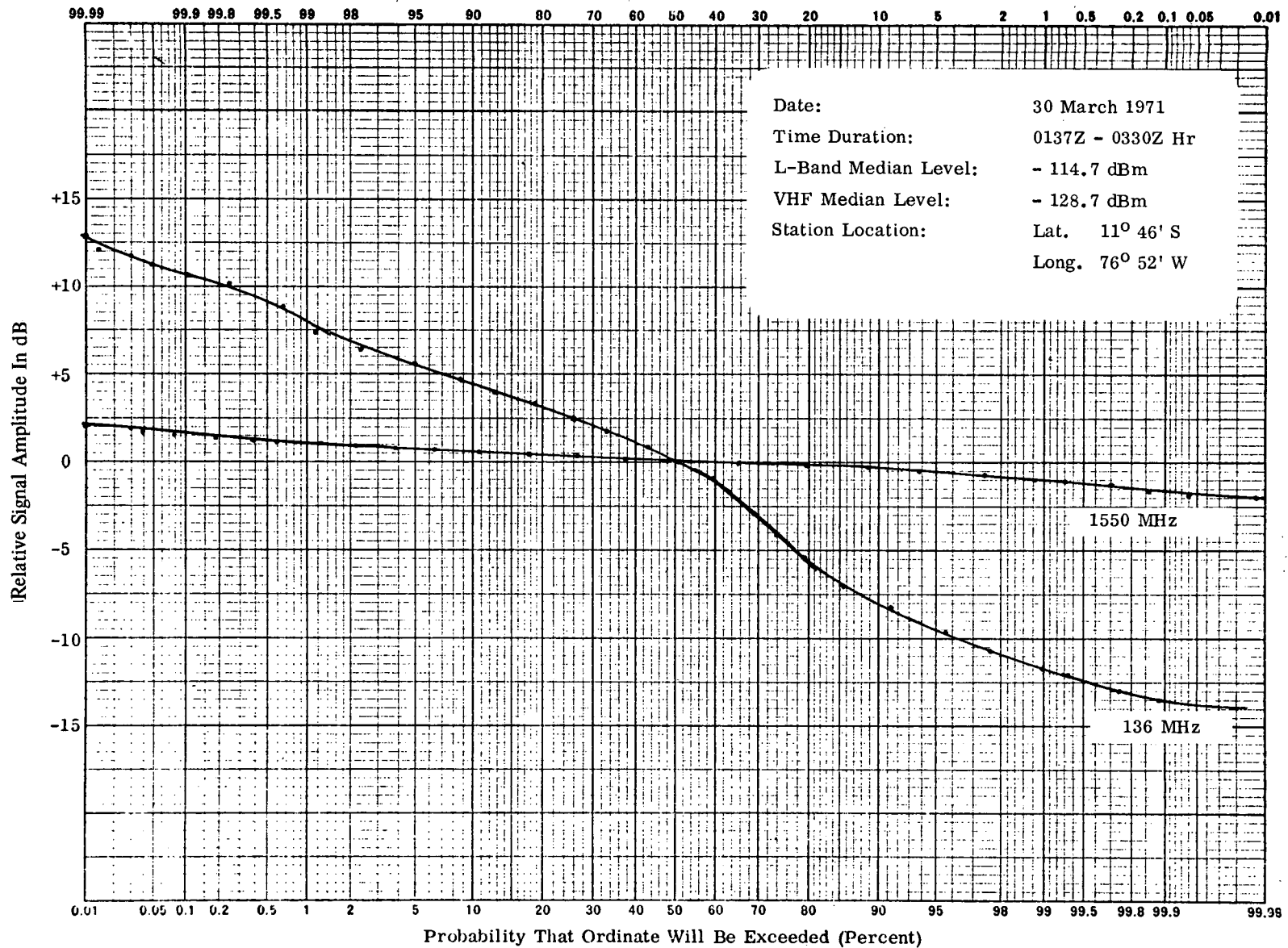


Figure 7. Cumulative Amplitude Distribution of ATS-5 L-Band and VHF Signals

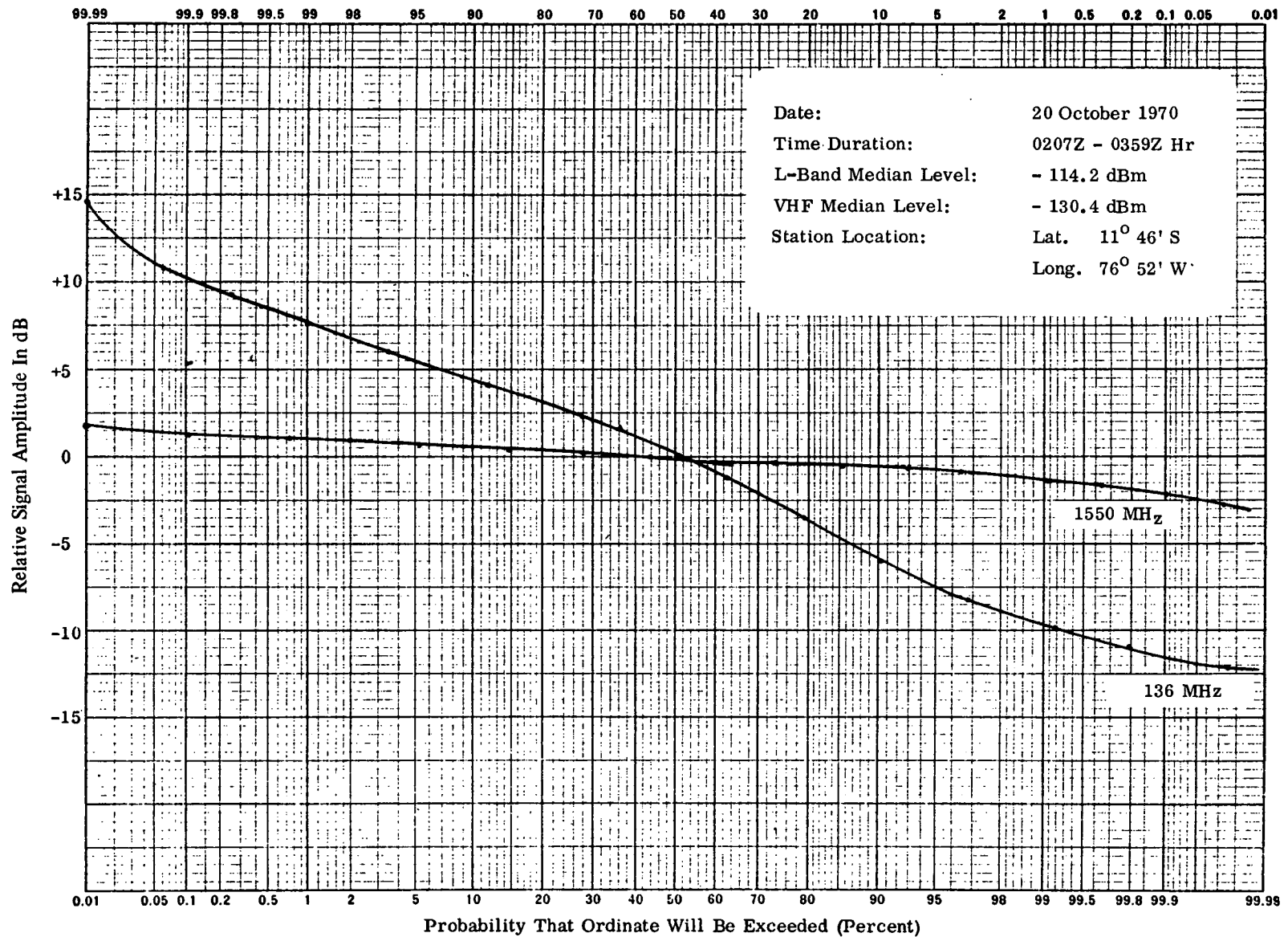


Figure 8. Cumulative Amplitude Distribution of ATS-5 and INTELSAT-1 Signals

DATE: 30 MARCH 1971
TIME: 0137Z - 0330Z

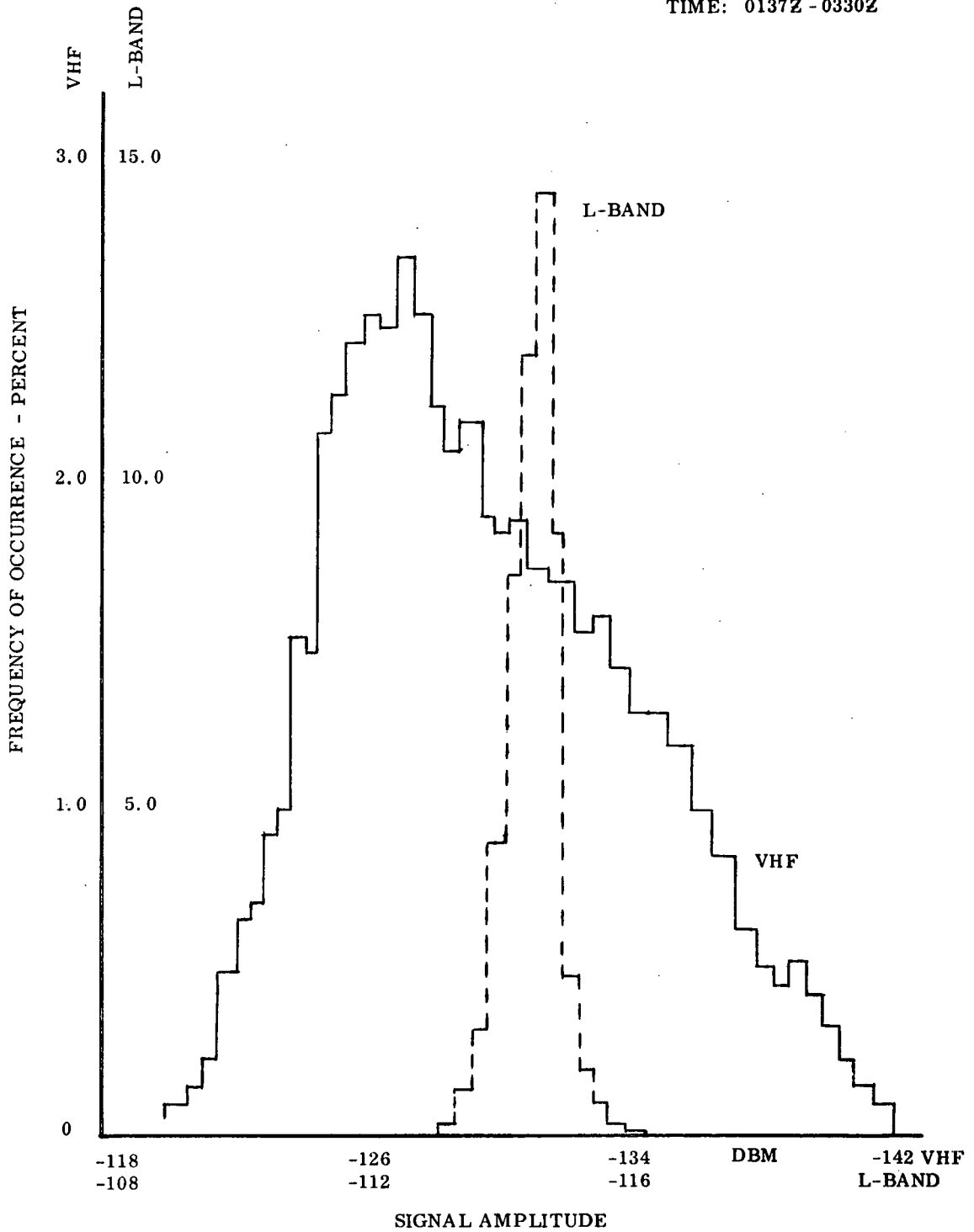


Figure 9. L-Band and VHF Distributions